J. Biochem. 124, 359-367 (1998)

Exchange of Nucleoside Monophosphate-Binding Domains in Adenylate Kinase and UMP/CMP Kinase[1]

Toshihide Okajima,*,[2] Tamo Fukamizo,* Sachio Goto,* Toshio Fukui,† and Katsuyuki Tanizawa†

*Faculty of Agriculture, Kinki University, 3327-204 Nakamachi, Nara 631-8505; and †Institute of Scientific and Industrial Research, Osaka University, Ibaraki, Osaka 567-0047

Received for publication, March 6, 1998

Two types of active chimeric enzymes have been constructed by genetic engineering of chicken cytosolic adenylate kinase (AK) and porcine brain UMP/CMP kinase (UCK): one, designated as UAU, carries an AMP-binding domain of AK in the remaining body of UCK; and the other, designated as AUA, carries a UMP/CMP-binding domain of UCK in the remaining body of AK. Steady-state kinetic analysis of these chimeric enzymes revealed that UAU is 4-fold more active for AMP, 40-fold less active for UMP, and 4-fold less active for CMP than the parental UCK, although AUA has considerably lowered reactivity for both AMP and UMP. Circular dichroism spectra of the two chimeric enzymes suggest that UAU and AUA have similar folding structures to UCK and AK, respectively. Furthermore, proton NMR measurements of the UCK and UAU proteins indicate that significant differences in proton signals are limited to the aromatic region, where an imidazole C2H signal assigned to His31 shows a downfield shift upon conversion of UCK to UAU, and the signals assigned to Tyr49 and Tyr56 in the UMP/CMP-binding domain disappear in UAU. In contrast, AUA has a T_m value about 11°C lower than AK, whereas UAU and UCK have similar T_m values. These results together show that the substrate specificity of nucleoside monophosphate (NMP) kinases can be engineered by the domain exchange, even though the base moiety of NMP appears to be recognized cooperatively by both the NMP-binding domain and the MgATP-binding core domain.

Key words: adenylate kinase, domain exchange, nucleoside monophosphate kinase, substrate specificity, UMP/CMP kinase.

Nucleoside monophosphate (NMP) kinases are ubiquitous enzymes, occurring in both prokaryotes and eukaryotes, and catalyze the reversible phosphoryl transfer between various nucleoside mono- and triphosphates in the salvage pathway of nucleotide metabolism (*1*). The NMP kinase family is further divided into subgroups consisting of adenylate kinases [EC 2.7.4.3] (AK), UMP (or UMP/CMP) kinases [EC 2.7.4.14] (UCK), guanylate kinases [EC 2.7.4.8], and thymidylate kinases [EC 2.7.4.9], on the basis of the differences in substrate specificity for NMP as a phosphoryl acceptor. For example, the enzymes in the AK subgroup are almost completely specific for AMP, and those in the UCK subgroup are highly specific for UMP and CMP. In marked contrast to the unique phosphoryl acceptor specificity of each subgroup, the phosphoryl donor specificity is not so high, with MgATP serving as the general substrate. Furthermore, X-ray crystallographic studies on several NMP kinases have revealed that they have essentially identical structures with a characteristic glycine-rich loop located in the N-terminal region (*2*), a common MgATP-binding "core" domain composed of the central 5-stranded parallel β-sheets surrounded by several α-helices, and a small, conserved NMP-binding domain (*3-6*) (Fig. 1). Among the NMP kinases, the enzymes of the AK subgroup have been most extensively studied in terms of their three-dimensional structures, interaction with substrates, and kinetic properties (*8-13*). Nevertheless, sufficient information for unequivocal understanding of the molecular basis of recognition of NMP substrates by NMP kinases is not yet available.

We previously reported that site-specific mutation of several residues (Thr39, Leu66, Val67, and Gln101) occurring in the putative AMP-binding domain of the chicken muscle AK (cytosolic isozyme) led to significant alteration of substrate specificity, rendering the enzyme more active for UMP and CMP than the wild-type enzyme (*13, 14*). We also cloned a cDNA coding for UCK from porcine brain and the recombinant enzyme was overproduced in *Escherichia coli* cells (*15*). Sequence comparison of the porcine brain UCK as well as those from other eukaryotes (*16, 17*) with the AK subgroup enzymes (par-

[1] This study was supported by a Grant-in-Aid for Scientific Research from the Ministry of Education, Science, Sports and Culture of Japan and a research grant from the Protein Research Foundation.

[2] To whom correspondence should be addressed. Tel: +81-742-43-1511, Fax: +81-742-43-1155, E-mail: okajima@nara.kindai.ac.jp

Abbreviations: AK, adenylate kinase; AP_5A, P^1,P^5-bis(5'-adenosyl)-pentaphosphate; DQF-COSY, double-quantum-filtered correlation spectroscopy; IPTG, isopropyl-β-D-thiogalactopyranoside; NMP, nucleoside monophosphate; NOESY, two-dimensional nuclear Overhauser effect spectroscopy; UCK, UMP/CMP kinase.

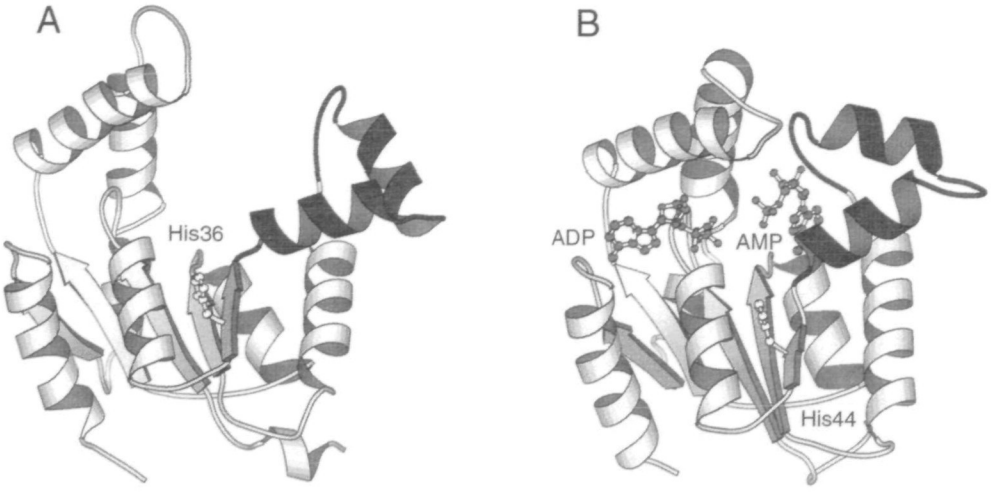

Fig. 1. **Schematic drawings of the three-dimensional structures of porcine cytosolic AK and yeast UMP kinase.** The figures were drawn by use of the program MOLSCRIPT (*7*) with the coordinates deposited in Protein Data Bank (ID codes; 3adk and 1ukz). (A) Porcine cytosolic AK in an open conformation without bound substrate (*3*) and (B) yeast UMP kinase in a closed conformation with ADP bound at the MgATP-binding site and AMP bound at the UMP-binding site (*6*). Side chains of His36 of the porcine AK and His44 of the yeast UMP kinase, both corresponding to His31 of the porcine UCK referred to in the text, as well as ADP and AMP molecules bound in the yeast UMP kinase are shown by a ball-and-stick model. The NMP-binding domains are shown in black.

ticularly the cytosolic enzymes from vertebrates) revealed the presence of highly conserved regions in the enzymes from the two different subgroups (*15*). Thus it was expected that AK and UCK would be good models for studying the mechanism by which NMP kinases recognize base moieties of NMP substrates. Along this line, we have constructed two types of active chimeric enzymes by genetic manipulation of the chicken cytosolic AK and the porcine brain UCK, between which the overall sequence identity is 41% (*15*). One chimeric enzyme, designated as UAU, carries the putative AMP-binding domain of AK in the remaining body of UCK, and the other, designated as AUA, carries the putative UMP/CMP-binding domain of UCK in the remaining body of AK. The results reported here clearly show that the specificity for NMP substrates of NMP kinases can actually be engineered by the domain exchange, even though the base moiety of NMP substrates appears to be recognized by not only the NMP-binding domain but also the MgATP-binding core domain.

EXPERIMENTAL PROCEDURES

Materials—The following materials were obtained commercially: nucleoside mono- and triphosphates (Seikagaku Kogyo or Sigma); lactate dehydrogenase and pyruvate kinase, both from rabbit muscle (Oriental Yeast); D_2O (99.8%) and Tris-d_6 (MSD Isotopes); vent DNA polymerase (New England Biolabs); cloning vectors pUC19 and M13tv19 (Takara Shuzo); and expression vectors pKK223-3 (Pharmacia) and pET-3b (Novagen). The original expression plasmid for the chicken muscle AK, pKK-cAK1-1 (*18*), was kindly provided by Drs. F. Kishi and A. Nakazawa, Yamaguchi University Medical School, from which the cDNA for the chicken muscle AK was subcloned into M13tv19. The expression plasmid pEUCK for the porcine brain UCK was described previously (*15*). All other chemicals were of the highest purity available.

Genetic Construction of Chimeric Enzymes—For construction of chimeric enzymes of AK and UCK, the genes coding for each enzyme were first amplified in three overlapping regions (AI-AIII and UI-UIII) by PCR with one of the following pairs of synthetic primers; P1+A3 for AI, A1+A4 for AII, A2+P2 for AIII, P3+U3 for UI, U1+U4 for UII, and U2+P1 for UIII. Among the amplified fragments, AII and UII correspond to the putative NMP-binding domain in AK and UCK, respectively, and others to the remaining flanking regions (Fig. 2).

A1: 5′-TATGG*C*TACACTCACCTCTC-3′
A2: 5′-CTGGTTCC*TCTAGA*CACGGTGCTGGACATG-3′
A3: 5′-GAGAGGTGAGTGTACCCATA-3′
A4: 5′-CGTGTC*TAGA*GGAACCAGCTCGCCTTCCTC-3′
U1: 5′-TATGG*G*TACAC*T*CACCTTTC-3′
U2: 5′-ATCGTGCC*TCTAGA*GATAACCATCAGTTTG-3′
U3: 5′-GA*G*AGGTG*A*GTGTAGCCATA-3′
U4: 5′-GTTATCTC*TAGA*GGCACGATCTTTCCATC-TTT-3′
P1: 5′-GTAAAACGACGGCCAGT-3′
P2: 5′-CTTGCATGCCTGCAGGTCGAC*A*CTAGAGG-ATCCCCGGGCCGT-3′
P3: 5′-CAGGAAACAGCTATGAC-3′

In the above primer sequences, the *Xba*I sites introduced for subsequent ligation of the amplified fragments are underlined, and mismatching bases are shown in italics. PCR was performed in a 50-μl solution containing 10 mM KCl, 10 mM $(NH_4)_2SO_4$, 20 mM Tris-HCl (pH 8.8), 2 mM $MgSO_4$, 0.1% Triton X-100, 0.2 mM each deoxynucleotide (dATP, dGTP, dCTP, and dTTP), 2 μM each primer, about 4 ng of the template DNA (M13tv19 containing the AK cDNA or pUC19 containing the UCK cDNA), and 4 units of vent DNA polymerase with a program consisting of 30 cycles of 94°C for 1 min, 55°C for 2 min, and 72°C for 3 min, and a final cycle of 94°C for 1 min, 55°C for 2 min, and 72°C for 13 min in a thermal cyclic reactor (Perkin Elmer, GeneAmp PCR System 2400). The PCR products were purified by agarose gel electrophoresis. To make the contiguous hybrid fragments AI-UII and UI-AII, a second PCR was done with AI and UII as a mixed template and the P1+U4 pair as primers for amplification of AI-UII, and with UI and AII as a mixed template and the P3+A4 pair as primers for amplification of UI-AII, under similar conditions as above.

After digestion with appropriate restriction enzymes,

these PCR fragments were cloned into pUC19 and their DNA sequences were confirmed with a Perkin Elmer 370S DNA sequencer; no undesired mutation was found in the amplified regions. Finally, the expression plasmid for AUA was constructed by connecting an *Eco*RI-*Xba*I fragment from AI-UII and an *Xba*I-*Pst*I fragment from AIII, followed by cloning into pKK223-3 to yield the plasmid designated as pKAUA. Similarly, the expression plasmid for UAU was constructed by connecting an *Sal*I-*Xba*I fragment from UI-AII and an *Xba*I-*Pst*I fragment from UIII, followed by cloning into pUC19, then insertion into pET-3b of a 0.6-kbp *Nde*I-*Bam*HI fragment excised from the resultant plasmid to yield the final expression plasmid designated as pTUAU.

Enzyme Purification—The wild-type AK and UCK were purified to homogeneity essentially as described previously (*15, 18*); the purified enzyme preparations were confirmed to be free from the endogenous AK produced in *E. coli* host cells, which accounts for less than 0.5% of the total AK activity in the crude extracts of the recombinant cells expressing the chicken muscle AK and is easily separated from the chicken muscle AK based on its inability to be adsorbed onto a phosphocellulose column (*18*). AUA was overproduced in *E. coli* JM109 cells harboring pKAUA by induction with 0.5 mM isopropyl-β-D-thiogalactopyranoside (IPTG). The chimeric enzyme recovered from the pellet of the cell lysate was purified by acid extraction and gel filtration as described previously for the insoluble site-specific mutant proteins of AK (*19*). UAU was overproduced in *E. coli* BL21 (DE3) cells harboring pTUAU by induction with 0.05 mM IPTG, and the chimeric enzyme was purified from the soluble fraction of the cell lysate by the same procedure as the wild-type UCK. All of the purified enzymes were concentrated by precipitation with ammonium sulfate, dialyzed against 30 mM Tris-HCl buffer (pH 7.5) containing 1 mM EDTA, 1 mM DTT, and 50% glycerol, and stored at −80°C until use.

Enzyme Assay and Steady-State Kinetic Analysis—The AK and UCK activities were measured by the standard assay methods as reported previously (*15, 19*). Steady-state kinetic analysis was performed by systematic variation of the concentrations of both MgATP as phosphoryl donor and AMP or UMP as phosphoryl acceptor in the coupled reaction mixture consisting of 87 mM triethanolamine-HCl buffer (pH 7.0), 10 mM $MgCl_2$, 100 mM KCl, 1 mM phosphoenolpyruvate, 0.16 mM NADH, 5 units of pyruvate kinase, and 20 units of lactate dehydrogenase. After preincubation at 25°C for about 2 min, an appropriate amount of enzyme was added to the mixture, and the reaction was carried out at 25°C. The decrease in absorbance at 340 nm due to the oxidation of NADH with pyruvate was monitored.

Measurement of Protein Concentration—The concentrations of the purified enzymes (AK, UCK, AUA, and UAU) were calculated from the absorbance at 280 nm using molar absorption coefficients of 10.7, 13.6, 13.4, and 10.9 $mM^{-1} \cdot cm^{-1}$, respectively, which were estimated from their amino acid compositions.

Proton NMR—For measuring ^{1}H-NMR spectra, the enzyme stock solution was dialyzed against 1 liter of 1 mM HEPES (pH 8.0), 50 mM KCl, 1 mM EDTA, and 1 mM DTT at 4°C for 16 h, and concentrated to about 40 mg/ml by use of an Amicon centricon-10 concentrator. The concentrated enzyme (600 μl) was lyophilized, dissolved in 1 ml of D_2O, lyophilized again, then dissolved in 600 μl of 50 mM Tris-d_6-DCl·D_2O buffer (pD 7.5, uncorrected) containing 1 mM DTT; insoluble proteins formed were removed by centrifugation. 1D NMR spectra were recorded at 500 MHz with a spectral width of 5,800.5 Hz using a JEOL GX-500 spectrometer. The HDO resonance was saturated by means of selective gated irradiation. The 2D phase-sensitive ^{1}H NMR spectra of double-quantum-filtered correlation spectroscopy (DQF-COSY) and two-dimensional nuclear Overhauser effect spectroscopy (NOESY) were also recorded at 500 MHz with a spectral width of 5,800.5 Hz in each dimension. A total of 48 scans were used for each of 256 t_1 values with 4,096 complex points in the ω_2 dimension. NOESY spectra were recorded with a 200-ms mixing time. All measurements were performed at 25°C, and ^{1}H chemical shifts were referenced to sodium 3-(trimethylsilyl)-propanesulfonic acid *via* the HDO resonance frequency at 4.76 ppm.

Thermal Stability—Thermal stabilities of the enzyme proteins were analyzed by monitoring the changes in ellipticity at 222 nm during the protein unfolding induced by heat with a Jasco model J-720 spectropolarimeter. All measurements were carried out in 5 mM sodium phosphate buffer (pH 7.2) containing 0.1 M NaCl, 1 mM EDTA, and 1 mM DTT at a protein concentration of 0.1 mg/ml. The temperature was raised continuously at a rate of 1°C/min through a thermostatic cell holder and was monitored with a Rikagaku Kogyo model DP-500 thermometer. The reversibility of protein unfolding was examined by measuring the ellipticity after gradual lowering of the temperature to 25°C.

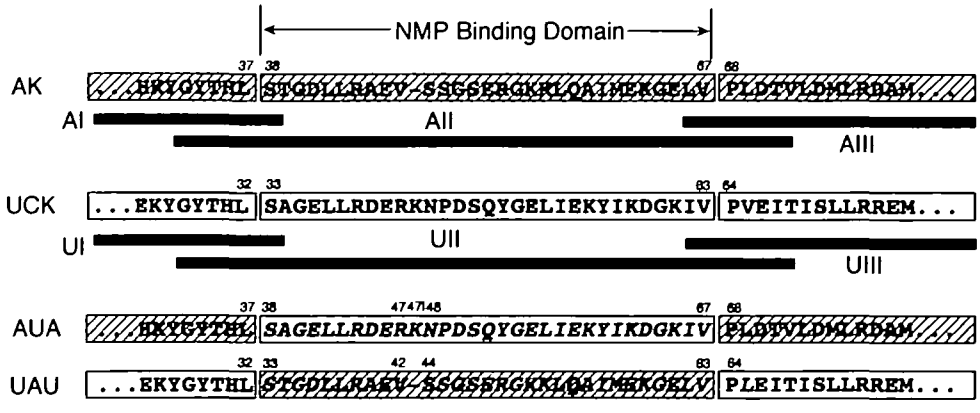

Fig. 2. **Amino acid sequences of NMP-binding domains and schematic representation of the PCR-amplified fragments.** The regions derived from AK are hatched. Residue numbers of the chimeric enzymes are based on those of the parental enzymes. Substituted residues are indicated by italic letters. The amplified DNA fragments are shown by thick bars. See text for details.

RESULTS

Construction and Purification of Chimeric Enzymes—The putative NMP-binding domains (*15, 20, 21*) of AK and UCK (see Fig. 1) were exchanged by a PCR-assisted method (Fig. 2) to examine their roles in the recognition of NMP bases and to attempt to interchange their substrate specificities. In AUA, the AMP-binding domain (residues 38-67) of AK was replaced by the UMP/CMP-binding domain (residues 33-63) of UCK. In UAU, the UMP/CMP-binding domain plus Val65 of UCK was replaced by the AMP-binding domain plus Leu69 of AK (introduction of an *Xba*I site, needed for the subsequent gene manipulations, led to the additional change; see Fig. 2). The expression level of the constructed UAU gene in *E. coli* cells was comparable to that of the parental UCK gene as judged by SDS-PAGE of the soluble fraction from the cell lysate (data not shown), and the overproduced UAU protein could be purified by the same procedure as the wild-type UCK (*15*). In the case of the AUA gene, the expression level was also relatively high, but most of the protein was found in the insoluble fraction of the cell lysate. Therefore, AUA was first solubilized by acid treatment, then purified by gel filtration as described previously for some insoluble site-specific mutant proteins of AK (*19*). All the purified enzymes were essentially homogeneous on SDS-PAGE (data not shown).

Substrate Specificity and Kinetic Constants—When measured under the standard assay conditions with 1 mM MgATP as phosphoryl donor and 1 mM AMP, UMP, or CMP as phosphoryl acceptor, AUA showed considerably decreased activities for both AMP and CMP, while maintaining the minuscule activity for UMP of the parental AK (Table I). In contrast, UAU was 4-fold more active for AMP, 40-fold less active for UMP, and 4-fold less active for CMP than the parental UCK (Table I). Thus, the substrate specificity of UCK was dramatically altered to that of AK by substituting the putative AMP-binding domain of AK into the remaining part of the UCK molecule. The failure of the such alteration from AK to UCK (as AUA) may be related to the conformational instability of AUA (see below) and its insolubility in the recombinant *E. coli* cells as described above.

Steady-state kinetic parameters of the two chimeric enzymes (UAU and AUA) as well as of the parental wild-type enzymes (UCK and AK) have been determined with each of MgATP-AMP and MgATP-UMP substrate pairs based on a random quasi-equilibrium Bi-Bi mechanism (Scheme 1), as previously reported for AK (*12*). In the scheme, K_{m1} and K_{m4} represent the Michaelis constants for an NMP substrate at zero and infinite concentrations of the other substrate MgATP, respectively, and K_{m2} and K_{m3} are those for MgATP at zero and infinite concentrations of an NMP substrate, respectively (*13*). If the phosphoryl transfer is the rate-limiting step in the forward reaction and all the other equilibria are adjusted rapidly (*22*), then the initial reaction rate (v) is given by Eqs. 1 and 2 using these Michaelis constants and the maximum rate (k_{cat}) obtained at infinite concentrations of both MgATP and an NMP substrate (*23*). Steady-state kinetic parameters calculated by the nonlinear regression method using the program SEQUEN described by Cleland (*24*) are summarized in Tables II and III.

$$v=\frac{k_{cat}}{1+\frac{K_{m4}}{[NMP]}+\frac{K_{m3}}{[MgATP]}+\frac{K_{m2}K_{m4}}{[NMP][MgATP]}} \quad (1)$$

$$K_{m1}K_{m3}=K_{m2}K_{m4} \quad (2)$$

When the kinetic values in the phosphoryl transfer from MgATP to AMP are compared (Table II), it is noteworthy that the wild-type UCK has very low K_m values even for the nonfavored substrate AMP (K_{m1} and K_{m4}), comparable to those of the wild-type AK. Therefore, the low reactivity for AMP of UCK (Table I) is ascribable only to its low k_{cat} value. As for UAU, although the K_m values for AMP became very high, the k_{cat} value in the MgATP-AMP reaction is much increased, resulting in nearly 4-fold increase in the specific activity for AMP, as compared with the parental UCK (Table I). On the other hand, the lowered specific activity of AUA in the MgATP-AMP reaction (Table I) is due to the combination of both the increases in the K_m values for AMP and the decrease in the k_{cat} value (Table II). The K_m values for MgATP (K_{m2} and K_{m3}) do not

TABLE I. **Specificity for NMP substrates.** Activities were measured at 25°C by the standard assay method with 1 mM MgATP and 1 mM AMP, UMP, or CMP. The ratios of specific activities for an NMP to those for AMP are shown in parentheses.

Enzyme	Specific activity (units/mg)		
	AMP	UMP	CMP
UCK	12 (1)	310 (26)	80 (6.7)
UAU chimera	44 (1)	7.7 (0.18)	19 (0.43)
AUA chimera	7.7 (1)	0.10 (0.013)	0.6 (0.078)
AK	950 (1)	0.075 (0.00008)	2.9 (0.003)

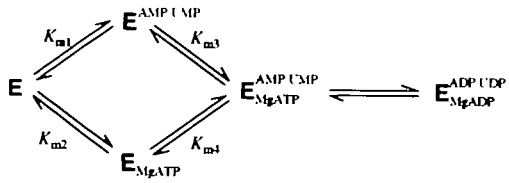

Scheme 1

TABLE II. **Kinetic parameters in the MgATP-AMP reaction.**

Enzyme	K_{m1} (mM)	K_{m2} (mM)	K_{m3} (mM)	K_{m4} (mM)	k_{cat} (s^{-1})	$k_{cat}/\sqrt{K_{m1}K_{m3}}$[a] ($s^{-1}\cdot M^{-1}$)	β[b]
UCK	0.50	0.27	0.11	0.20	4.99	21.7	2.5
UAU chimera	3.78	0.14	0.25	6.82	99.7	102	0.55
AUA chimera	3.64	0.36	1.00	10.2	35.1	18.3	0.36
AK	0.42	0.28	0.11	0.17	467	2,120	2.5

[a]Defined catalytic efficiency ($=k_{cat}/\sqrt{K_{m2}K_{m4}}$). [b]Simplified cooperativity factor ($=K_{m1}/K_{m4}=K_{m2}/K_{m3}$).

change significantly among UCK, UAU, AUA, and AK, except for the nearly 10-fold increase in the K_{m3} value of AUA. Catalytic efficiencies including substrate specificity factors, defined as $k_{cat}/\sqrt{K_{m1}K_{m3}}$ ($=k_{cat}/\sqrt{K_{m2}K_{m4}}$), also correlate well with the specific activities of each enzyme (Tables I and II).

When the kinetic values in the phosphoryl transfer from MgATP to UMP are compared (Table III), it is evident that only the wild-type UCK has low K_m values for UMP (K_{m1} and K_{m4}) and a large k_{cat} value. Substitution of the AMP-binding domain for the UMP/CMP-binding domain in UCK (as UAU) indeed led to rigorous impairment of the UMP-binding properties (*i.e.*, increase in K_{m1} and K_{m4} values) and considerable decrease in the k_{cat} value. However, the reversal (substitution of the UMP/CMP-binding domain for the AMP-binding one in AK, as AUA) also failed to lower the K_m values for UMP and to raise the k_{cat} value. The K_m values for MgATP (K_{m2} and K_{m3}) of the chimeric enzymes are again changed little, by less than 3-fold (Table III), as compared with each parental enzyme (*cf.* UCK *vs.* UAU and AK *vs.* AUA).

Tables II and III also include the calculated simplified cooperativity factors, β ($=K_{m1}/K_{m4}=K_{m2}/K_{m3}$), for substrate binding (*12*), which define the extent of increase in affinities for the second substrate (K_{m3} and K_{m4}) after binding of the first substrate (either MgATP or AMP/UMP). Thus, if $\beta>1.0$, the substrate binding is positively cooperative; if $\beta=1.0$, uncooperative; and if $\beta<1.0$, negatively cooperative. Positive cooperativity for substrate binding has been observed with AK (*12*) and is believed to be mediated by allosteric conformational changes induced upon binding of either first substrate (*22*) (see also Fig. 1). Our present kinetic data indicate that UCK shows positive cooperativity most prominently with UMP as phosphoryl acceptor, whereas UAU, AUA, and AK show weak or no cooperativities with UMP (Table III). With AMP as phosphoryl acceptor, UAU and AUA show even negative cooperativities (Table II). It is possible that the decreases in the allosteric cooperativity (β values) are derived from the reduced rates of conformational changes and, if the main rate-determining step is in the conformational changes, they account at least partly for the low k_{cat} values.

CD Spectra—The CD spectra in the far UV region (200-250 nm) derived from the main chain folding of UAU and AUA were comparable to those of the parental UCK and AK, respectively (Fig. 3). The mean residue ellipticities (θ) at 222 nm of UCK and UAU were about -1.8×10^4 deg·cm^2·dmol^{-1}, and those of AK and UAU were about -1.2×10^4 deg·cm^2·dmol^{-1}. These findings suggest that both chimeric enzymes fold into main chain structures similar to those of their parental enzymes. In other words, the introduced NMP-binding domains are presumably accommodated without affecting the overall structures of the stepmother enzymes. The catalytic activities of the chimeric enzymes, being reduced though, also support this; enzymatic activities are sensitive criteria for correct folding of engineered proteins.

Thermal Stability—Conformational stabilities of AK, UCK, AUA, and UAU were analyzed by monitoring the thermal unfolding process following the changes in ellipticity at 222 nm. Thermal unfolding parameters calculated according to the method of Pace *et al.* (*25*) are summarized in Table IV; reversibilities of the unfolding process were

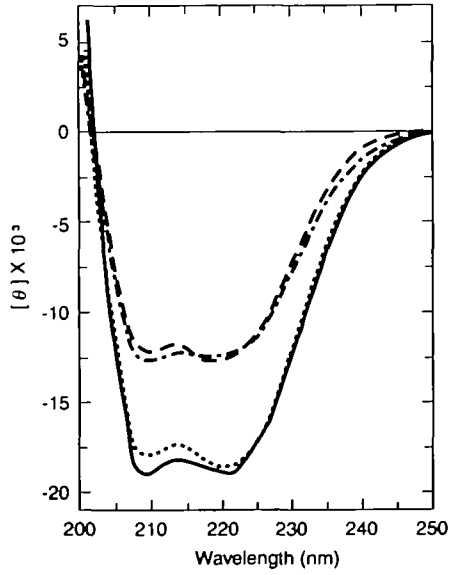

Fig. 3. **CD spectra of AK, AUA, UCK, and UAU in the far-UV region.** CD spectra were measured at a protein concentration of 0.2 mg/ml at 25°C and pH 7.5; UCK (—), UAU (·····), AK (- - -), and AUA ( ).

TABLE IV. **Thermal unfolding parameters.** Thermodynamic parameters for the thermal unfolding process were determined by monitoring the changes in ellipticity (θ) at 222 nm as described under "EXPERIMENTAL PROCEDURES." T_m represents the temperature at the midpoint of the unfolding transition. The thermal transition curve was analyzed by assuming the two-state approximation of N (native)⇄D (unfolded), and the equilibrium constant of unfolding ($K_D=[D]/[N]$) was determined from the equation $K_D=f_D/(1-f_D)$, where f_D is the fraction of the unfolded molecule at each temperature. Enthalpy and entropy changes (ΔH and ΔS) at T_m were determined from the van't Hoff plot.

Enzyme	T_m (°C)	ΔH at T_m (kcal/mol)	ΔS at T_m (kcal/mol/deg)
UCK	51.4	66.8	0.206
UAU chimera	52.3	57.1	0.175
AUA chimera	49.6	62.1	0.192
AK	60.2	73.3	0.220

TABLE III. **Kinetic parameters in the MgATP-UMP reaction.**

Enzyme	K_{m1} (mM)	K_{m2} (mM)	K_{m3} (mM)	K_{m4} (mM)	k_{cat} (s^{-1})	$k_{cat}/\sqrt{K_{m1}K_{m3}}$[a] ($s^{-1}\cdot M^{-1}$)	β[b]
UCK	0.45	0.26	0.034	0.059	174	1,450	7.6
UAU chimera	10.8	0.14	0.086	6.53	13.7	14.3	1.6
AUA chimera	32.7	0.47	0.42	29.0	0.65	0.18	1.1
AK	55.7	0.38	0.23	34.1	1.61	0.45	1.6

[a]Defined catalytic efficiency ($=k_{cat}/\sqrt{K_{m2}K_{m4}}$). [b]Simplified cooperativity factor ($=K_{m1}/K_{m4}=K_{m2}/K_{m3}$).

50-70% for all the four enzymes. Although ΔH and ΔS values of UAU are considerably smaller than those of the parental UCK, its T_m value is similar to that of UCK, indicating that the replacement of the NMP-binding domain did not affect the thermal stability of UCK. Conversely, the domain exchange in AK to AUA reduced the thermal stability of AK, lowering the T_m value by about 11°C.

Proton NMR Spectra—UAU shows an altered substrate specificity but possesses similar main chain folding and thermal stability to the parental UCK, as described above. To further detail the structural changes caused by the domain replacement, we measured 1D and 2D ^{1}H-NMR spectra of UCK and UAU. 1D ^{1}H-NMR spectra of the enzymes uncomplexed or complexed with a bi-substrate analog, P^1,P^5-bis(5′-adenosyl)pentaphosphate (AP_5A), in the presence of $MgCl_2$ are shown in Fig. 4; UAU showed 1D ^{1}H-NMR spectra very similar to those of UCK in the aliphatic region (0.0-3.5 ppm) with or without AP_5A and $MgCl_2$. Significant differences in the proton signals were limited to the aromatic region (6.2-8.2 ppm) of the spectra.

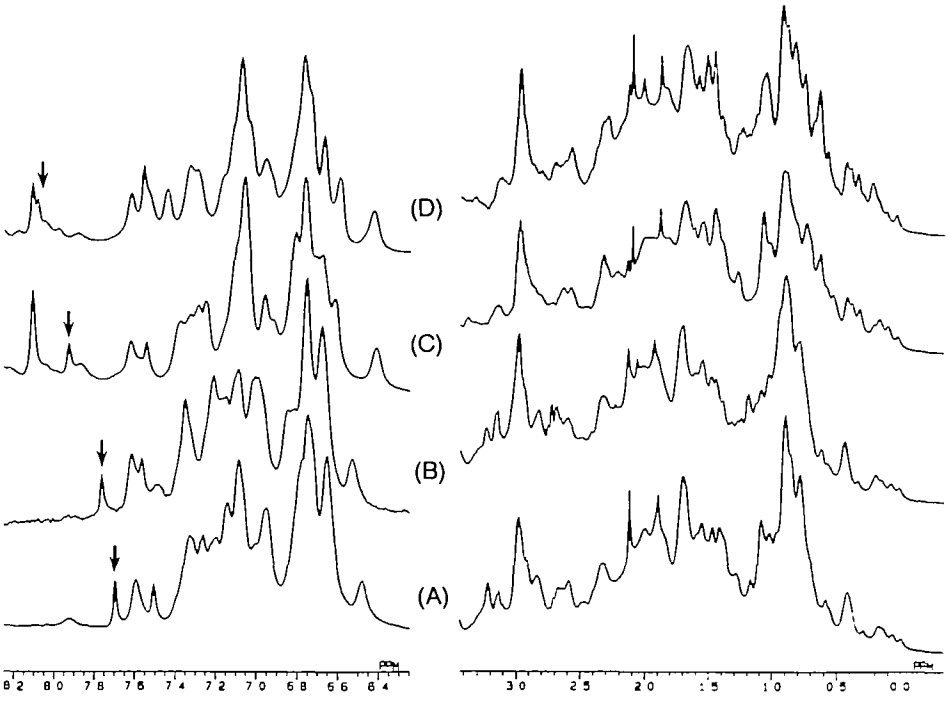

Fig. 4. **1D ^{1}H-NMR spectra of UCK and UAU.** ^{1}H-NMR spectra were measured at 25°C and pH 7.5; right, aliphatic region; left, aromatic region. (A) 1.2 mM UCK, (B) 0.73 mM UAU, (C) 2.4 mM UCK with 8 mM $MgCl_2$ and 5.8 mM AP_5A, and (D) 2.0 mM UAU with 8 mM $MgCl_2$ and 4.4 mM AP_5A. The C2H signals of His31 are indicated by arrows.

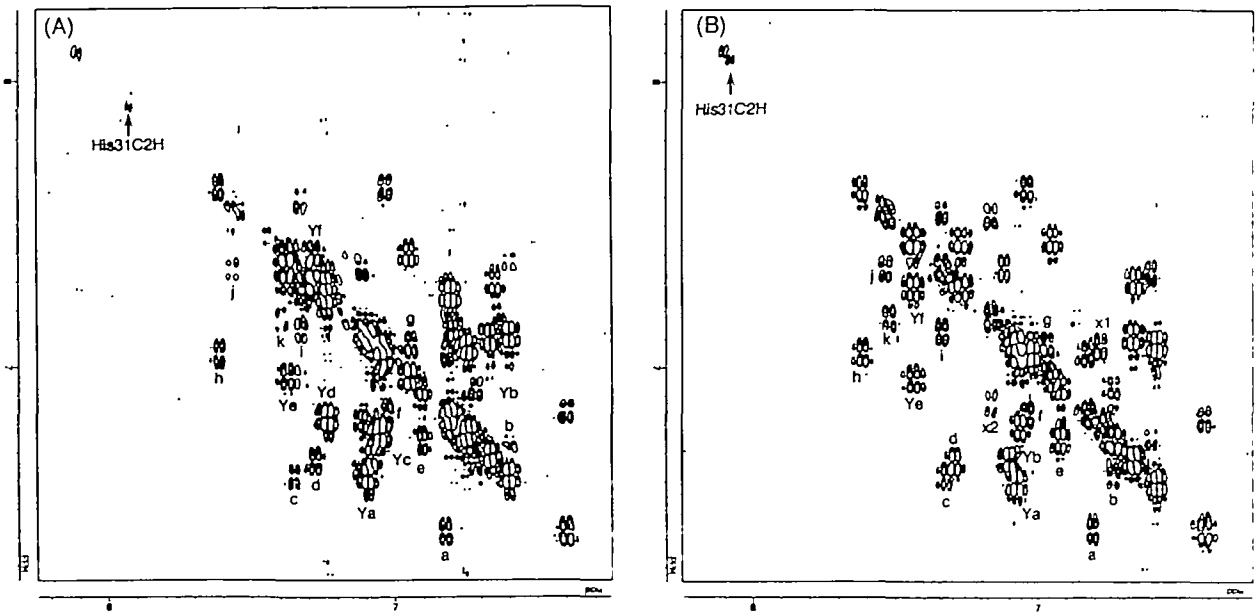

Fig. 5. **DQF-COSY spectra of UCK and UAU complexed with AP_5A.** DQF-COSY spectra of UCK (A) and UAU (B) were measured at 25°C and pH 7.5 with the same samples used in Fig. 4, (C) and (D), respectively.

It is suggested that the major differences arise from disappearance of the signals of two Tyr residues (Tyr49 and Tyr56 in UCK), as a result of the replacement of the UMP/CMP-binding domain with the AMP-binding domain, which contains no Tyr residues (see Fig. 2). Therefore, we attempted to assign each signal to the aromatic residues by comparing 2D ^{1}H-NMR spectra. Because the uncomplexed UCK and UAU readily aggregated and precipitated, particularly at high protein concentrations (above about 1 mM) during a long period of 2D ^{1}H-NMR measurement (beyond about 16 h), we measured 2D ^{1}H-NMR spectra of the enzymes complexed with AP_5A and $MgCl_2$, which stabilized both proteins and prevented their aggregation during the NMR measurements.

Aromatic regions of the DQF-COSY spectra of UAU and UCK complexed with AP_5A are shown in Fig. 5, and chemical shifts of all the well-isolated signals are summarized in Table V. We undertook signal assignments on the basis of the connectivities of the DQF-COSY and NOESY spectra, but weakness and complexities of a number of signals allowed us to identify only partially the spin systems in UCK and UAU. For example, in the aromatic region of the DQF-COSY spectra of UCK (Fig. 5A), we found six typical cross peaks due to six Tyr residues. In the UAU spectra (Fig. 5B), four spin systems were assigned to four Tyr residues. The two signals designated as Yc and Yd in the DQF-COSY spectrum of UCK disappeared in the spectrum of UAU and hence are assignable to Tyr49 and Tyr56 in the UMP/CMP-binding domain of UCK.

Furthermore, sharp signals at 7.93 and 8.09 ppm were assigned to the imidazole C2H proton of His31 in UCK and UAU complexed with AP_5A, respectively, both of which contain a single His residue, and the assignment is consistent with their narrow signal line widths. The C2H signals of His31 showed the largest change in chemical shifts (Δ = 0.16 ppm, downfield) upon conversion of UCK to UAU (Table V). Also, the chemical shifts of the C2H signals in the uncomplexed UCK and UAU (sharp singlet signals at 7.70 and 7.76 ppm, respectively, in the 1D ^{1}H-NMR spectra; see Fig. 4) moved upfield concomitantly with the increase in the solvent pH (data not shown). From the pH dependency of the chemical shifts, pK_a values of His31 were estimated to be 6.05 and 5.55 in the uncomplexed UCK and UAU, respectively. These results suggest that the electrostatic environment around His31 of UAU is perturbed by the domain replacement. Because His31 of UCK is probably located on the domain boundary, facing the NMP-binding domain (*3, 6*) (see Fig. 1), and the uncomplexed UCK should be in an open conformation (*20*) with the pK_a value of His31 being close to that of the free histidine ($pK_a = 6.0$), the introduced AMP-binding domain in UAU presumably causes structural perturbation that affects the pK_a of His31 (lowering in a 0.5 pH unit). The UAU molecule might be to some extent already in a closed conformation in the absence of substrates (and AP_5A), and this suggestion is compatible with the weak or negative cooperativities for substrate binding of UAU (refer to β values in Tables II and III). As shown in Fig. 5 and Table V, changes in the chemical shifts of the other signals in the 2D ^{1}H-NMR spectra of UCK and UAU are less than 0.04 ppm, except for those designated as Ye, Yf, and k. Consequently, aromatic residues contained in the region other than the NMP-binding domain are not much structurally perturbed and the domain replacement appears to affect only the fine structure of the domain boundary region.

TABLE V. **Chemical shifts of the signals detected in the DQF-COSY spectra.** The chemical shifts were determined from the DQF-COSY spectra shown in Fig. 5. Differences in chemical shift between UCK/AP_5A and UAU/AP_5A are shown in parentheses.

Signal	UCK/AP_5A (ppm)		UAU/AP_5A (ppm)	
Ya	6.61	7.10	6.58 (−0.03)	7.08 (−0.02)
Yb	6.67	7.09	6.67 (0)	7.10 (0.01)
Yc	6.76	7.06	ND[a]	
Yd	6.81	7.25	ND[a]	
Ye	6.96	7.39	6.95 (−0.01)	7.44 (0.05)
Yf	7.24	7.39	7.26 (0.02)	7.44 (0.05)
His31C2H	7.93		8.09 (0.16)	
a	6.41	6.84	6.42 (0.01)	6.82 (−0.02)
b	6.61	6.73	6.61 (0)	6.74 (0.01)
c	6.61	7.36	6.61 (0)	7.32 (−0.04)
d	6.65	7.29	6.66 (0.01)	7.30 (0.01)
e	6.72	6.92	6.74 (0.02)	6.92 (0)
f	6.82	7.04	6.82 (0)	7.04 (0)
g	6.95	7.07	6.97 (0.02)	7.08 (0.01)
h	7.03	7.62	7.04 (0.01)	7.61 (−0.01)
i	7.12	7.34	7.11 (−0.01)	7.34 (0)
j	7.33	7.57	7.33 (0)	7.54 (−0.03)
k	7.17	7.40	7.16 (0.01)	7.52 (0.12)
x1	ND[b]		6.78	7.07
x2	ND[c]		6.86	7.17

[a]Not detected. [b]Not detected due to overlapping with other signals. [c]Not detected, probably due to signal weakness.

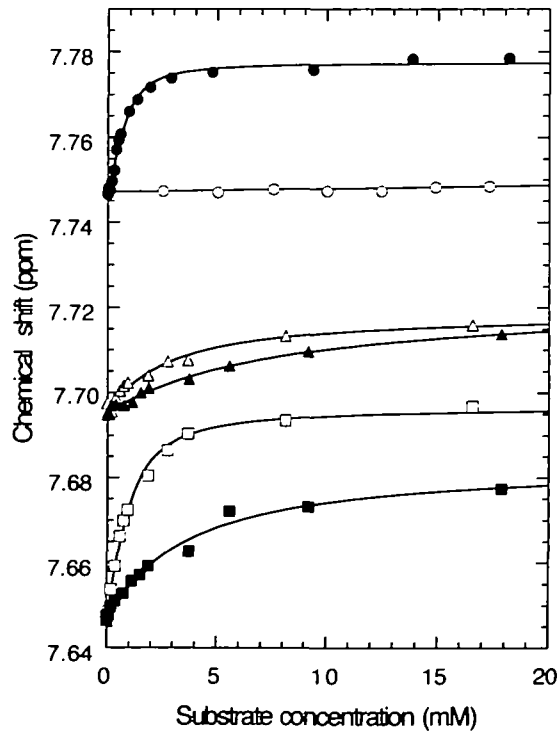

Fig. 6. **Effect of NMP concentrations on the chemical shifts of the C2H signals of His36 (AK) and His31 (UCK and UAU).** The chemical shift was plotted against the concentration of AMP (●) and UMP (○) for AK; AMP (■) and UMP (□) for UCK; and AMP (▲) and UMP (△) for UAU. Curves were fitted to the data by the nonlinear least square method.

TABLE VI. **Dissociation constants for UMP and AMP determined from the downfield changes in chemical shift of the C2H signals of His31 (UCK and UAU) and His36 (AK) upon ligand binding.** The data shown in Fig. 6 were fitted by the nonlinear least square method for calculation of the K_d values.

Enzyme	Ligand	K_d (mM)	$\Delta\delta^a$ (ppm)
UCK	UMP	0.44	0.050
	AMP	3.2	0.036
UAU chimera	UMP	2.5	0.023
	AMP	7.3	0.026
AK	UMP	No binding	No binding
	AMP	0.40 (0.50)[b]	0.033

[a]Maximum changes in chemical shift at infinite concentration of the ligand. [b]Determined by Sanders *et al.* (*10*) according to the binding model at the ligand-enzyme molar ratio of 2.

Substrate Binding—It has been reported that the imidazole C2H proton signal of His36 of AK, corresponding to His31 of UCK (and also of UAU), moves downfield upon addition of substrate AMP (*10*). Therefore, to determine dissociation constants (K_d) for NMP substrates of UCK, UAU, and AK by 1D ^{1}H-NMR measurements of the downfield movements, each enzyme was titrated with AMP or UMP and the chemical shift of the C2H signal was plotted against substrate concentration (Fig. 6). The C2H signal of His31 of UCK and UAU moved downfield to different extents upon addition of AMP or UMP. The corresponding His36 signal of AK was also moved downfield by the addition of AMP, as reported previously (*10*), but no change in the chemical shift was detected upon addition of UMP. As shown in Fig. 6, the observed chemical shifts were well fitted by the nonlinear least square method to the theoretical curves obtained based on the assumption that the enzyme binds stoichiometrically an NMP ligand (*i.e.*, at a molar ratio of 1:1). The calculated K_d values are summarized in Table VI. The K_d values of UCK for UMP and of AK for AMP agreed nearly completely with the K_{m1} values determined kinetically (Tables II and III), which denote K_m values for the first-bound NMP substrate. However, the other K_d values (of UCK for AMP, of UAU for UMP and AMP, and of AK for UMP) did not accord with their respective K_{m1} values.

DISCUSSION

The results described in this paper, particularly those with the UAU chimera, demonstrate that the exchange of the NMP-binding domains between the two homologous NMP kinases is more advantageous for engineering their substrate specificities than the site-specific mutagenesis of individual residues directly involved in binding of the NMP bases, as previously reported for a mutant enzyme of AK, in which Thr39 was replaced by Ala (*14*). Thus, in terms of the catalytic efficiencies ($k_{cat}/\sqrt{K_{m1}K_{m3}}$; Tables II and III), the chimeric enzyme UAU constructed by the domain exchange is 7-fold more reactive for AMP than for UMP, whereas the parental UCK is about 70-fold more reactive for its preferred substrate UMP than for AMP. This marked change in the substrate preference far exceeds that attained with the site-specific AK mutant, which still retains much higher reactivity for the original substrate AMP than for UMP or CMP (*14*).

As described earlier, the NMP kinases have essentially identical three-dimensional structures (*3-6*), and they undergo substantial conformational changes upon substrate binding (*3-6, 8, 9*). The structures of porcine cytosolic AK in an open conformation without bound substrate (*3*) and yeast UMP kinase in a closed conformation bound with ADP at the MgATP-binding site and AMP at the UMP-binding site (*6*) are shown schematically in Fig. 1, A and B, respectively; they are homologues of chicken cytosolic AK and porcine brain UCK, respectively, used in the present studies. Since the binding site for the base moiety of NMP substrates is located in the small domain, apart from the MgATP-binding core domain (Fig. 1B), the exchange of NMP-binding domains between the two enzymes is not expected to significantly affect MgATP-binding properties. Indeed, K_{m2} and K_{m3} values for MgATP of the chimeric enzymes were changed only by 2-3-fold from those of their parental enzymes, although the K_{m3} value for MgATP of AUA was considerably large (Tables II and III). However, K_m values for AMP and UMP (K_{m1} and K_{m4}) of the chimeric enzymes increased unexpectedly. Thus, these results suggest that the base moiety of NMP substrates is recognized by not only the NMP-binding domain alone but also a part of the MgATP-binding core domain, as a result of conformational changes induced by substrate binding.

The catalytic efficiency of UAU for AMP is still much lower than that of the natural enzyme AK (Table II). This again suggests that the catalytic efficiency for a particular NMP substrate is determined by a combination of the NMP-binding domain and other regions of the core domain such as those involved in the conformational changes or the phosphoryl transfer. Supporting this suggestion is the fact that, in the X-ray crystallographic structures of several NMP kinases complexed with an NMP substrate or its analog (*4-6, 8*), the base moiety of NMP is bound to the NMP-binding domain and also to a part of the core domain facing it (Fig. 1B). Therefore, the specificities for NMP substrates are probably determined through the cooperative recognition of the nucleotide base by several residues assembled after the conformational changes (*8*). Also, the fact that UAU containing the AMP-binding domain of AK has a larger K_d value for AMP than UCK (Table VI) supports the interpretation that the NMP-binding domain alone is insufficient for recognition of an NMP base. Furthermore, it is likely that, even though the NMP-binding domain itself contains no residues directly involved in the catalysis, slight changes in the binding mode of an NMP substrate would affect the optimum positioning of catalytic residues of the core domain relative to the α-phosphate group of the bound NMP that accepts the γ-phosphate group of MgATP, leading to the decrease in k_{cat} values. Finally, the decreases in the cooperativity factors (β values) for substrate binding that resulted from the domain exchange (Tables II and III) and site-directed mutagenesis (*12, 13*) would also delineate an incorrect positioning of catalytic residues in the ternary complex (E/NMP/MgATP) needed for the optimum phosphoryl transfer reaction.

The fact that the UAU chimera and its parental UCK have similar folding structures as measured by CD and ^{1}H-NMR spectroscopies and similar thermal stabilities as judged from the T_m values suggests that the AMP-binding domain is well accommodated in the UCK structure to display the expected change in the specificity for NMP substrates. In contrast, the UMP/CMP-binding domain is

accepted by the AK structure only with accompanying decreases in thermal stability and solubility in *E. coli* cells. Obviously, the structural perturbation in AUA seems to be too extensive for the enzyme to exhibit high catalytic efficiencies. The fact that UCK has a wider specificity for NMP substrates than AK (see Table I) may correlate with the structural flexibility of UCK, allowing the exchange of the NMP-binding domains.

In conclusion, the present studies clearly demonstrate that the specificity of NMP kinases for NMP substrates can be engineered by means of domain exchange. Both the UMP/CMP- and AMP-binding domains were shown to be functional in catalyzing the respective base-specific phosphoryl transfer when connected with the remaining part of the UCK structure.

We thank Drs. F. Kishi and A. Nakazawa for providing plasmid pKK-cAK1-1, and Y. Iwai and S. Imai for their technical assistance.

REFERENCES

1. Anderson, E.P. (1973) Nucleoside and nucleotide kinases in *The Enzymes* (Boyer, P.D., ed.) Vol. 9, pp. 49-96, Academic Press, Orlando, FL
2. Walker, J.E., Saraste, M., Brunswick, M.J., and Gay, N.J. (1982) Distantly related sequences in the α- and β-subunits of ATP-synthase, myosin, kinases and other ATP-requiring enzymes and a common nucleotide binding fold. *EMBO J.* **1**, 945-951
3. Dreusicke, D., Karplus, P.A., and Schulz, G.E. (1988) Refined structure of porcine cytosolic adenylate kinase at 2.1 Å resolution. *J. Mol. Biol.* **199**, 359-371
4. Diederichs, K. and Schulz, G.E. (1991) The refined structure of the complex between adenylate kinase from beef heart mitochondrial matrix and its substrate AMP at 1.85 Å resolution. *J. Mol. Biol.* **217**, 541-549
5. Stehle, T. and Schulz, G.E. (1992) Refined structure of the complex between guanylate kinase and its substrate GMP at 2.0 A resolution. *J. Mol. Biol.* **224**, 1127-1141
6. Müller-Dieckmann, H.-J. and Schulz, G.E. (1995) Substrate specificity and assembly of the catalytic center derived from two structures of ligated uridylate kinase. *J. Mol. Biol.* **246**, 522-530
7. Kraulis, P.J. (1991) MOLSCRIPT: A program to produce both detailed and schematic plots of protein structure. *J. Appl. Cryst.* **26**, 946-950
8. Müller, C.W. and Schulz, G.E. (1992) Structure of the complex between adenylate kinase from *Escherichia coli* and the inhibitor Ap_5A refined at 1.9 Å resolution. *J. Mol. Biol.* **224**, 159-177
9. Berry, M.B., Meador, B., Bilderback, T., Liang, P., Glaser, M., and Phillips, N.P., Jr. (1994) The closed conformation of a highly flexible protein: the structure of *E. coli* adenylate kinase with bound AMP and AMPPNP. *Proteins: Struct. Funct. Genet.* **19**, 183-198
10. Sanders, C.R., II, Tian, G., and Tsai, M.-D. (1989) Mechanism of adenylate kinase. Is there a relationship between local substrate dynamics, local binding energy, and the catalytic mechanism? *Biochemistry* **28**, 9028-9043
11. Byeon, I.-J.L., Yan, H., Edison, A.S., Mooberry, E.S., Abildgaard, F., Markley, J.L., and Tsai, M.-D. (1993) Mechanism of adenylate kinase. ^1H, ^{13}C, and ^{15}N NMR assignments, secondary structures, and substrate binding sites. *Biochemistry* **32**, 12508-12521
12. Okajima, T., Tanizawa, K., Yoneya, T., and Fukui, T. (1991) Role of leucine 66 in the asymmetric recognition of substrates in chicken muscle adenylate kinase. *J. Biol. Chem.* **266**, 11442-11447
13. Okajima, T., Tanizawa, K., and Fukui, T. (1993) Site-directed random mutagenesis of AMP-binding residues in adenylate kinase. *J. Biochem.* **114**, 627-633
14. Okajima, T., Tanizawa, K., and Fukui, T. (1993) Site-directed mutagenesis of AMP-binding residues in adenylate kinase: Alteration of substrate specificity. *FEBS Lett.* **334**, 86-88
15. Okajima, T., Goto, S., Tanizawa, K., Tagaya, M., Fukui, T., Shimofuruya, H., and Suzuki, J. (1995) Cloning, sequencing, and expression in *Escherichia coli* of a cDNA encoding porcine brain UMP-CMP kinase. *J. Biochem.* **117**, 980-986
16. Liljelund, P., Sanni, A., Friesen, J.D., and Lacroute, F. (1989) Primary structure of the *S. cerevisiae* gene encoding uridine monophosphokinase. *Biochem. Biophys. Res. Commun.* **165**, 464-473
17. Wiesmüller, L., Noegel, A.A., Bârzu, O., Gerisch, G., and Schleicher, M. (1990) cDNA-derived sequence of UMP-CMP kinase from *Dictyostelium discoideum* and expression of the enzyme in *Escherichia coli*. *J. Biol. Chem.* **265**, 6339-6345
18. Tanizawa, Y., Kishi, F., Kaneko, T., and Nakazawa, A. (1987) High level expression of chicken muscle adenylate kinase in *Escherichia coli*. *J. Biochem.* **101**, 1289-1296
19. Tagaya, M., Yagami, T., Noumi, T., Futai, M., Kishi, F., Nakazawa, A., and Fukui, T. (1989) Site-directed mutagenesis of Pro-17 located in the glycine-rich region of adenylate kinase. *J. Biol. Chem.* **264**, 990-994
20. Schulz, G.E., Müller, C.W., and Diederichs, K. (1990) Induced-fit movements in adenylate kinases. *J. Mol. Biol.* **213**, 627-630
21. Müller-Dieckmann, H.-J. and Schulz, G.E. (1994) The structure of uridylate kinase with its substrates, showing the transition state geometry. *J. Mol. Biol.* **236**, 361-367
22. Tian, G., Yan, H., Jiang, R.-T., Kishi, F., Nakazawa, A., and Tsai, M.-D. (1990) Mechanism of adenylate kinase. Are the essential lysines essential? *Biochemistry* **29**, 4296-4304
23. Hamada, M. and Kuby, S.A. (1978) Studies on adenosine triphosphate transphosphorylases. XIII. Kinetic properties of the crystalline rabbit muscle ATP-AMP transphosphorylase (adenylate kinase) and a comparison with the crystalline calf muscle and liver adenylate kinases. *Arch. Biochem. Biophys.* **190**, 772-779
24. Cleland, W.W. (1979) Statistical analysis of enzyme kinetic data. *Methods Enzymol.* **63**, 103-138
25. Pace, C.N., Shirley, B.A., and Thomson, J.A. (1989) Measuring the conformational stability of a protein in *Protein Structure: A Practical Approach* (Creighton, T.E., ed.) pp. 311-330, IRL Press, Oxford